Queen's University Belfast

Robustness of Damping Control Implemented by Energy Storage Systems Installed in Power Systems

Wang, H., Du, W., Chen, S. J., Wen, J. Y., & Dunn, R. (2011). Robustness of Damping Control Implemented by Energy Storage Systems Installed in Power Systems. International Journal of Electrical Power and Energy Systems, 33 (1)(1), 35-42. DOI: 10.1016/j.ijepes.2010.08.006

Published in:
International Journal of Electrical Power and Energy Systems

Queen's University Belfast - Research Portal:
Link to publication record in Queen's University Belfast Research Portal

General rights
Copyright for the publications made accessible via the Queen's University Belfast Research Portal is retained by the author(s) and / or other copyright owners and it is a condition of accessing these publications that users recognise and abide by the legal requirements associated with these rights.

Take down policy
The Research Portal is Queen's institutional repository that provides access to Queen's research output. Every effort has been made to ensure that content in the Research Portal does not infringe any person's rights, or applicable UK laws. If you discover content in the Research Portal that you believe breaches copyright or violates any law, please contact openaccess@qub.ac.uk.

Download date:15. Feb. 2017

Electrical Power and Energy Systems 33 (2011) 35–42

Contents lists available at ScienceDirect

Electrical Power and Energy Systems

journal homepage: www.elsevier.com/locate/ijepes

Robustness of damping control implemented by Energy Storage Systems installed in power systems

W. Du [a,b,*], H.F. Wang [b], S. Cheng [c], J.Y. Wen [c], R. Dunn [d]

[a] The Southeast University, Nanjing, China
[b] The Queen's University of Belfast, Belfast, UK
[c] Huazhong University of Science and Technology, China
[d] The University of Bath, Bath, UK

ARTICLE INFO

Article history:
Received 26 August 2008
Received in revised form 14 June 2010
Accepted 13 August 2010

Keywords:
Energy Storage System (ESS)
Power system oscillations
Equal-area criterion
Small-signal stability analysis
BESS and SMES

ABSTRACT

An Energy Storage System (ESS) installed in a power system can effectively damp power system oscillations through controlling exchange of either active or reactive power between the ESS and power system. This paper investigates the robustness of damping control implemented by the ESS to the variations of power system operating conditions. It proposes a new analytical method based on the well-known equal-area criterion and small-signal stability analysis. By using the proposed method, it is concluded in the paper that damping control implemented by the ESS through controlling its active power exchange with the power system is robust to the changes of power system operating conditions. While if the ESS damping control is realized by controlling its reactive power exchange with the power system, effectiveness of damping control changes with variations of power system operating condition. In the paper, an example of power system installed with a battery ESS (BESS) is presented. Simulation results confirm the analytical conclusions made in the paper about the robustness of ESS damping control. Laboratory experiment of a physical power system installed with a 35 kJ/7 kW Superconducting Magnetic Energy Storage (SMES) was carried out to evaluate theoretical study. Results are given in the paper, which demonstrate that effectiveness of SMES damping control realized through regulating active power is robust to changes of load conditions of the physical power system.

© 2010 Elsevier Ltd. All rights reserved.

1. Introduction

In addition to the advantage of being able to accommodate the intermittence of renewable generation, an Energy Storage System (ESS) installed in a power system can help to enhance system stability by regulating its exchange of active and reactive power with the power system. Superconducting Magnetic Energy Storage (SMES), Battery Energy Storage System (BESS), Flywheel Energy Storage (FES), and Pumped Storage Hydro Power Station (PSHPS) are commonly used ESS in power system stability control [1–3]. To investigate and validate the capability of those ESS in one of the important applications of stability control – to suppress power system oscillations, various tools and techniques have been used, such as the modal analysis based on linearized models for SMES [4–8], modeling power electronics into power systems for BESS [9–11], simulation and laboratory experiment for FES [12] as well as application of advanced control theory for BESS [13,14]. Research results obtained so far indicate that ESS control can significantly enhance power system stability by damping system oscillations effectively, which has been confirmed by field applications of BESS and PSHPS reported in [15] and [16] respectively.

This paper investigates the robustness of damping control implemented by ESS to variations of power system operating conditions. The focus of investigations is to study the difference of ESS damping control when it is realized by controlling exchange of either active or reactive power between ESS and power system. The paper proposes a new analytical method for the small-signal analysis of ESS control to damp power system oscillations based on the linearized equal-area criterion. By using the proposed method, it is demonstrated in the paper that effectiveness of ESS damping control realized by regulating exchange of active power does not change with variations of power system operating conditions; while it does when ESS damping control is realized by regulating exchange of reactive power. Hence ESS damping control is more robust to variations of power system operating conditions if it is implemented through regulating exchange of active power than via controlling exchange of reactive power. In the paper, an example power system installed with a BESS is presented. Simulation results of the example power system have confirmed analytical conclusions obtained. Laboratory experiment of a physical power

* Corresponding author. Address: School of Electrical Engineering, Southeast University, Nanjing, China.
E-mail addresses: ddwenjuan@gmail.com, jrest@anl.gov (W. Du).

0142-0615/$ - see front matter © 2010 Elsevier Ltd. All rights reserved.
doi:10.1016/j.ijepes.2010.08.006

system installed with a 35 kJ/7 kW SMES was also carried out to evaluate theoretical investigations. Results of experiment are given in the paper, which demonstrate that SMES damping control through regulating active power exchange is robust to load variations of the physical power system.

2. Robustness of ESS damping control

Fig. 1 shows a single-machine infinite-bus power system installed with a shunt-connected BESS, where X_s is the reactance of a step-down transformer and $\overline{V}_C$ is the voltage at the AC terminal of Voltage Source Converter (VSC) connected to the ESS. From Fig. 1 we can have

$$\begin{aligned}\overline{V}_S &= jX_{sb}\bar{I}_{sb} + \overline{V}_b = jX_{sb}\left[\bar{I}_{ts} - \left(\frac{\overline{V}_S - \overline{V}_C}{jX_S}\right)\right] + \overline{V}_b \\ &= jX_{sb}\bar{I}_{ts} - \frac{X_{sb}}{X_S}\overline{V}_S + \frac{X_{sb}}{X_S}\overline{V}_C + \overline{V}_b\end{aligned}$$

Hence

$$\overline{V}_S = \frac{jX_{sb}}{1+\frac{X_{sb}}{X_S}}\bar{I}_{ts} + \frac{X_{sb}}{X_S\left(1+\frac{X_{sb}}{X_S}\right)}\overline{V}_C + \frac{\overline{V}_b}{1+\frac{X_{sb}}{X_S}}$$

That gives

$$\begin{aligned}\overline{V}_t &= jX_{ts}\bar{I}_{ts} + \overline{V}_S \\ &= j\left(X_{ts} + \frac{X_S X_{sb}}{X_S + X_{sb}}\right)\bar{I}_{ts} + \frac{X_{sb}}{X_S + X_{sb}}\overline{V}_C + \frac{X_S}{X_S + X_{sb}}\overline{V}_b \\ &= jX\bar{I}_{ts} + \overline{V}\end{aligned} \tag{1}$$

where

$$X = \left(X_{ts} + \frac{X_S X_{sb}}{X_S + X_{sb}}\right), \quad \overline{V} = \frac{X_{sb}}{X_S + X_{sb}}\overline{V}_C + \frac{X_S}{X_S + X_{sb}}\overline{V}_b = a\overline{V}_C + b\overline{V}_b$$

From Eq. (1) we can obtain the active power delivered along the transmission line to be

$$P_{12} = \frac{V_t V}{X}\sin\theta \tag{2}$$

where θ is the angle between $\overline{V}_t$ and $\overline{V}$, as it is shown by the phasor diagram of Fig. 2.

The focus of investigation in this paper is the dynamic exchange of active and reactive power between the ESS and power system. No matter what type of ESS is and how the ESS is modeled in details, variations of phase and magnitude, V_C and γ, of voltage, $\overline{V}_C$, can exactly represent the exchange of active and reactive power separately. Hence in the following discussion, robustness of ESS

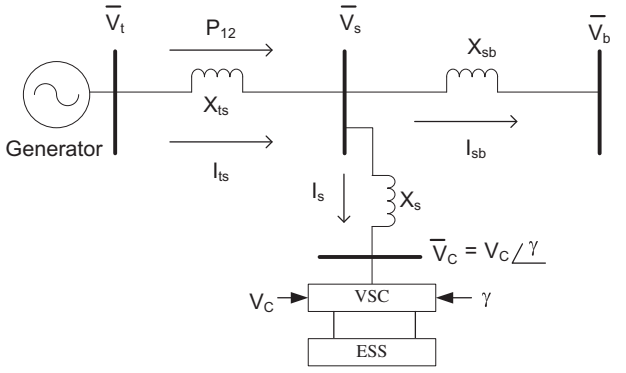

Fig. 1. A single-machine infinite-bus power system installed with a shunt-connected BESS.

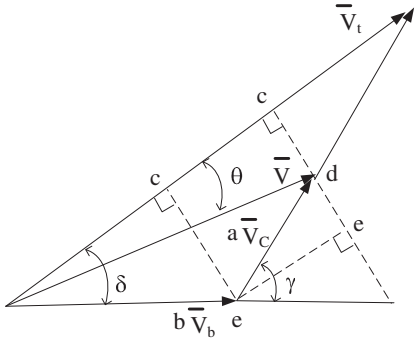

Fig. 2. Phasor diagram.

damping control will be studied by examining the forced variations of V_C and γ due to ESS control. From Fig. 2 we have

$$cd = V\sin\theta = ce - de = bV_b\sin\delta + aV_C\sin(\gamma - \delta)$$

By using Eq. (2) we have

$$P_{12} = \frac{V_t}{X}[bV_b\sin\delta + aV_C\sin(\gamma - \delta)] = f(\delta, V_C, \gamma) \tag{3}$$

Hence small-signal variation (oscillation) of active power delivered along the transmission line is

$$\Delta P_{12} = \Delta P_{12thita} + \Delta P_{Econtrol} \tag{4}$$

where $\Delta P_{12thita} = \frac{\partial P_{12}}{\partial\delta}C_{12thita}\Delta\delta$ is the variation of active power caused by deviation of δ and $\Delta P_{Econtrol} = \frac{\partial f}{\partial V_C}\Delta V_C + \frac{\partial f}{\partial\gamma}\Delta\gamma$ is the forced variation due to ESS control. If $\Delta P_{Econtrol} = C_{Cthita}\Delta\delta + C_{CDthita}\Delta\dot{\delta}$ (decomposed in $\Delta\delta - \Delta\dot{\delta}$ co-ordinate), we have

$$\Delta P_{12} = \Delta P_{12thita} + \Delta P_{12Dthita} \tag{5}$$

where $\Delta P_{12thita} = (C_{12thita} + C_{Cthita})\Delta\delta$ and $\Delta P_{12Dthita} = C_{CDthita}\Delta\dot{\delta}$. The small-signal analysis given in Appendix A of the paper shows that the effectiveness of ESS damping control is determined by the value of coefficient, $C_{CDthita}$. The higher $C_{CDthita}$ is, the better damping effect is achieved by ESS control.

By observing Eq. (1), it can be seen that the power system with the ESS installed is electrically equivalent to a single-machine infinite-bus power system without the ESS installed where the equivalent line reactance is X and voltage at the infinite busbar is $\overline{V}$. Hence the active power delivered along the transmission line can be written as

$$\begin{aligned}P_{12} &= \frac{E'_q V}{x'_{d\Sigma}}\sin\theta - \frac{(x_q - x'_d)V^2}{x'_{d\Sigma}x_{q\Sigma}}\sin 2\theta \\ &= \frac{E'_q}{x'_{d\Sigma}}[bV_b\sin\delta + aV_c\sin(\delta - \gamma)] \\ &\quad - \frac{(x_q - x'_d)}{x'_{d\Sigma}x_{q\Sigma}}[bV_b\sin\delta + aV_c\sin(\delta - \gamma)][bV_b\cos\delta \\ &\quad + aV_c\cos(\delta - \gamma)] \\ &\approx \frac{E'_q}{x'_{d\Sigma}}[bV_b\sin\delta + aV_c\sin(\delta - \gamma)]\end{aligned} \tag{6}$$

where θ is the angle between E'_q and $\overline{V}$.

As it is pointed out above, ESS control can realize the exchange of both active and reactive power between the ESS and power system. This is implemented by controlling the modulation ratio and phase of VSC, V_C and γ, respectively. Usually there is an established voltage control function by the ESS to regulate the voltage profile at the ESS AC terminal. Damping control function can be either superimposed on the ESS voltage control or through regulating the modulation phase γ directly. For the simplicity of analysis,

we assume that a proportional damping control law is adopted and damping feedback signal is the rotor speed of the generator (if a locally available signal, such as the active power delivered along the transmission line, is used, it can always be represented as the linear combination of rotor angle and rotor speed. This will not change the discussion below). Hence damping control superimposed on ESS voltage control function is

$$V_c = V_{c0} + K_{vol}(V_{sref} - V_s) + K_{dampV}(\omega - 1)$$

This is to control the exchange of reactive power between the ESS and power system to realize ESS damping control function. Linearization of the above equation gives

$$\Delta V_c = -K_{vol}\Delta V_s + K_{dampV}\Delta\omega$$

From Eq. (A1) in Appendix B we can obtain

$$\Delta V_c = \frac{-K_{vol}C_1}{1 + K_{vol}C_2}\Delta\delta - \frac{K_{dampV}}{1 + K_{vol}C_2}\Delta\omega \tag{7}$$

Hence from Eqs. (4)–(7) we have

$$\Delta P_{Econtrol} = C_{Cthita}\Delta\delta + C_{CDthita}\Delta\omega \tag{8}$$

where

$$C_{CDthita} = -\frac{E'_{q0}}{X'_{d\Sigma}} aV_{c0}\sin(\delta_0 - \gamma_0)\frac{K_{dampV}}{1 + K_{vol}C_2}$$

From the above equation we can see that $C_{CDthita}$ changes with variations of system load condition. At a heavier load condition with higher $\delta_0 - \gamma_0$, $C_{CDthita}$ is higher and hence ESS damping control is more effective.

If ESS damping control function is implemented by regulating γ directly instead of superimposing it on the ESS voltage control, it means damping control is achieved via exchange of active power between the ESS and power system. We have

$$V_c = V_{c0} + K_{vol}(V_{sref} - V_s); \quad \gamma = \gamma_0 + K_{damp\gamma}(\omega - 1)$$

Hence we have the linearized control law to be

$$\Delta V_c = -K_{vol}\Delta V_s; \quad \Delta\gamma = K_{damp\gamma}\Delta\omega \tag{9}$$

From Eqs. (9) and (A1) in Appendix B we can obtain

$$\Delta V_c = \frac{-K_{vol}C_1}{1 + K_{vol}C_2}\Delta\delta - \frac{K_{vol}C_3}{1 + K_{vol}C_2}K_{damp\gamma}\Delta\omega \tag{10}$$

From Eqs. (4), (5), (6), and (10) we have

$$\Delta P_{Econtrol} = C_{Cthita}\Delta\delta + C_{CDthita}\Delta\omega \tag{11}$$

where

$$C_{CDthita} = \frac{E'_{q0}}{X'_{d\Sigma}} aV_{c0}K_{damp\gamma}\left[\sin(\delta_0 - \gamma_0)\frac{K_{vol}C_3}{1 + K_{vol}C_2} + \cos(\delta_0 - \gamma_0)\right]$$

Similarly, by observing the coefficient $C_{CDthita}$ in Eq. (11) we can see that because $\cos(\delta_0 - \gamma_0)$ decreases and $\sin(\delta_0 - \gamma_0)$ increases at a higher load condition (higher $\delta_0 - \gamma_0$), overall $C_{CDthita}$ may not change much with the variation of system load conditions. This

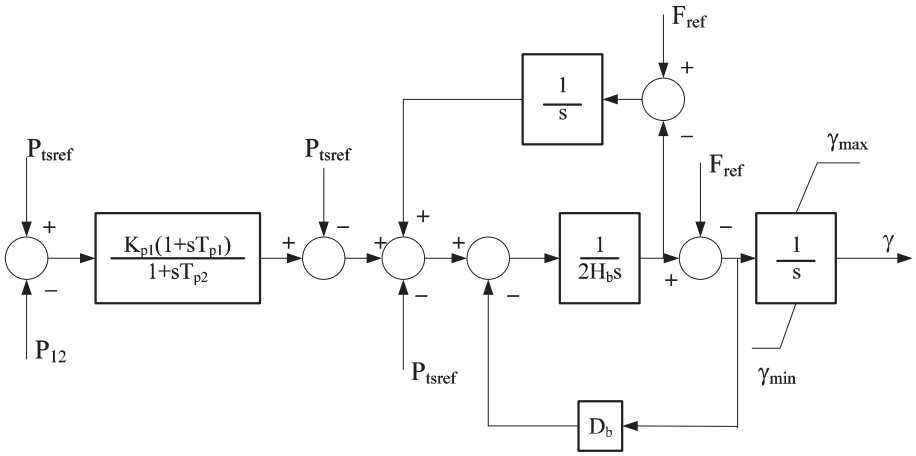

Part (a)

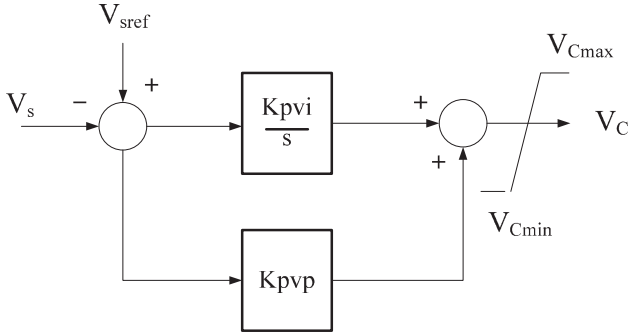

Part (b)

Fig. 3. Dynamic model of BESS used in simulation study.

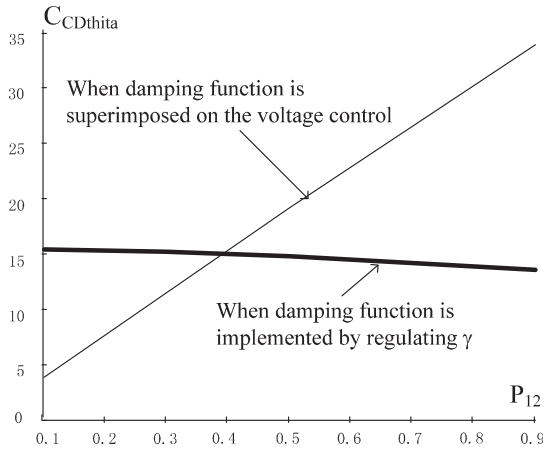

Fig. 4. $C_{CDthita}$ with variation of system load conditions.

means ESS damping control is of better robustness to the changes of system load conditions when it is implemented by regulating γ than by superimposing it on the ESS voltage control function.

3. Simulation study

An example single-machine infinite-bus power system installed with a BESS was used for simulation study. Parameters of the system are given in Appendix C. Full non-linear system model and dynamic model of the BESS in [17] are used. Fig. 3 shows the configuration of the BESS used in the study, where part (a) of the model is for the active power regulation and part (b) is that for the dynamic voltage support at the busbar where the BESS is installed. BESS is installed at the middle point of the transmission line connecting the generator and infinite busbar. From Fig. 3 we can see that a normal function of voltage regulation is implemented by a proportional–integral (PI) controller. Deviation of active power delivered along the transmission line is used as the feedback signal of BESS damping control. A PI damping controller was designed and added on the output of parts (a) and (b) of the BESS model separately to regulate the exchange of active and reactive power between the BESS and power system.

Fig. 4 shows the computational results of $C_{CDthita}$ with variation of system load conditions. From Fig. 4 we can see that $C_{CDthita}$ changes much less when BESS damping control is implemented by regulating γ (exchange of active power) than when it is superimposed on its voltage control (by regulating exchange of reactive

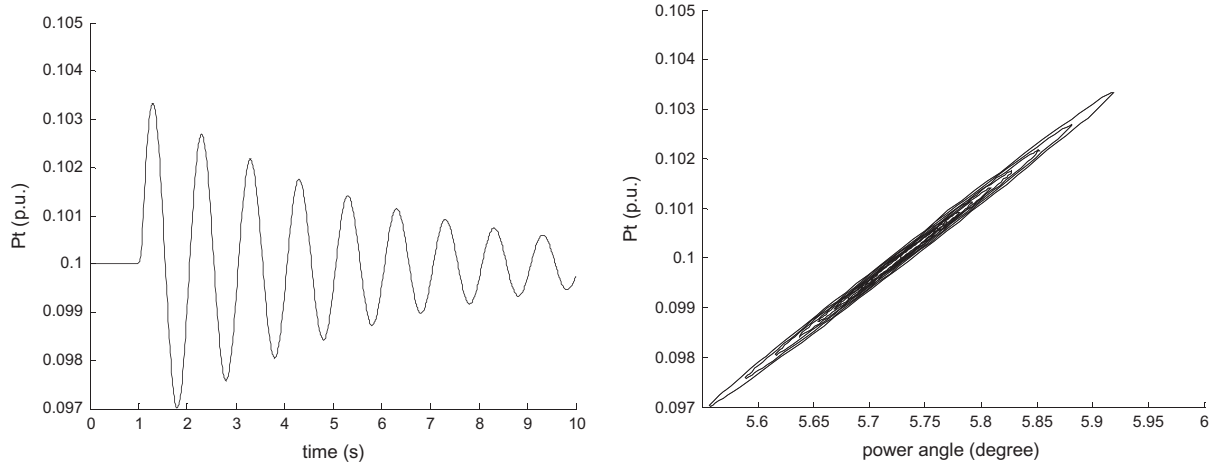

(a) $P_{12} = 0.1$p.u.

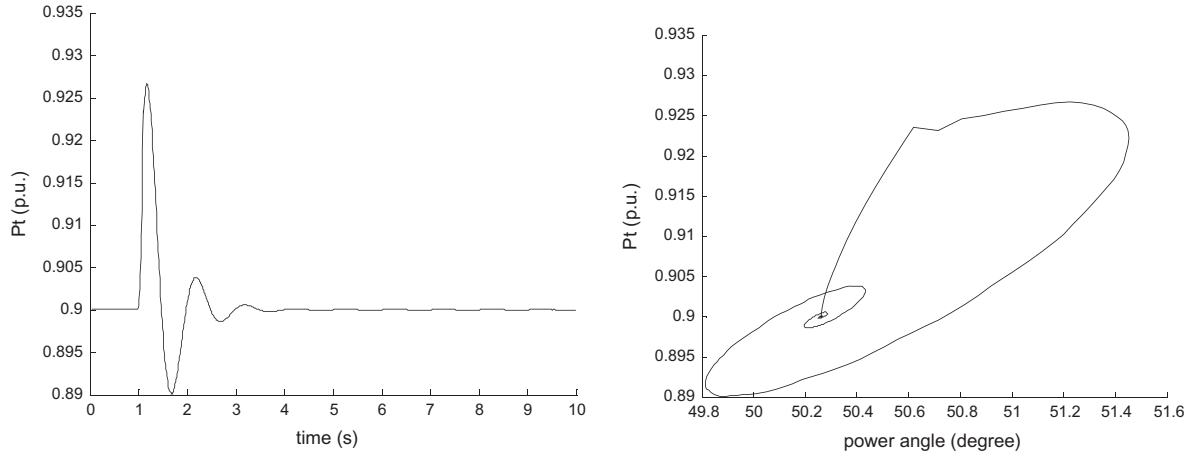

(b) $P_{12} = 0.9$p.u.

Fig. 5. Simulation results with BESS damping control superimposed on its voltage control at two different system load conditions.

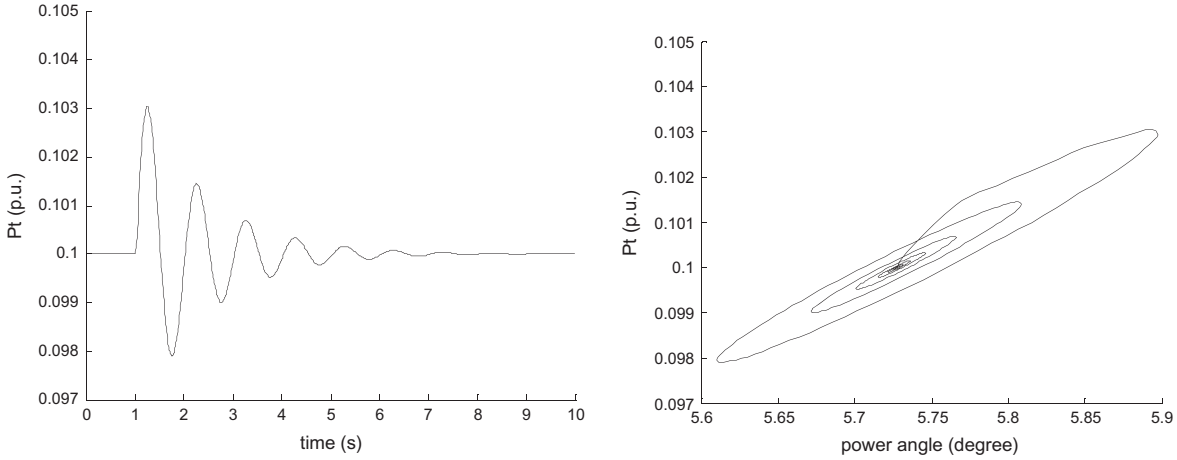

(a) $P_{12} = 0.1$p.u.

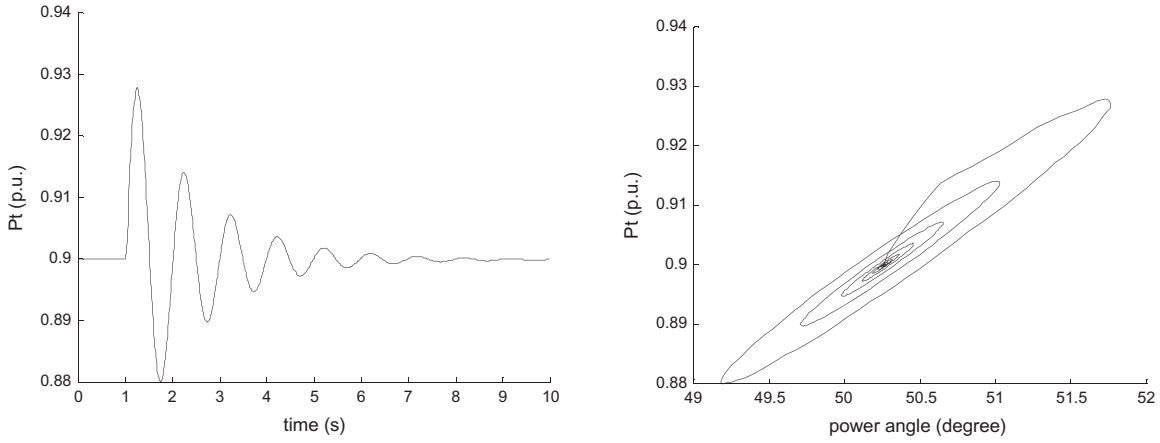

(b) $P_{12} = 0.9$p.u.

Fig. 6. Simulation results with BESS damping control implemented by regulating at two different load conditions.

power). This confirms analytical conclusions drawn in the above section when some simplifications for analysis are made.

Confirmation from the results of non-linear simulation is given in Figs. 5 and 6 at two different level of load flow conditions P_{12} = 0.1 p.u. and P_{12} = 0.9 p.u. Simulation started with the system subject to a small disturbance of 5% increase of mechanical input to the generator for 100 ms. Comparing two results in Fig. 5 we can see that at a higher load flow condition, BESS damping control is more effective when it is realized by regulating exchange of reactive power between the BESS and power system. From Fig. 6 we can see that effectiveness of BESS damping control does not change much with the variations of system load conditions. Therefore, those simulation results confirm the analytical conclusions that ESS damping control is more robust to variations of power system operating conditions when it is implemented though regulating exchange of active power between the ESS and power system.

4. Study of laboratory experiment

In order to further evaluate the theoretical analysis at a close-to-real environment, laboratory experiment was carried out at the Laboratory of Physical Power Systems, Wuhan University, China. The ESS used in the experiment is a 35 kJ/7 kW High Temperature Superconducting (HTS) dispersal module type of SMES, which

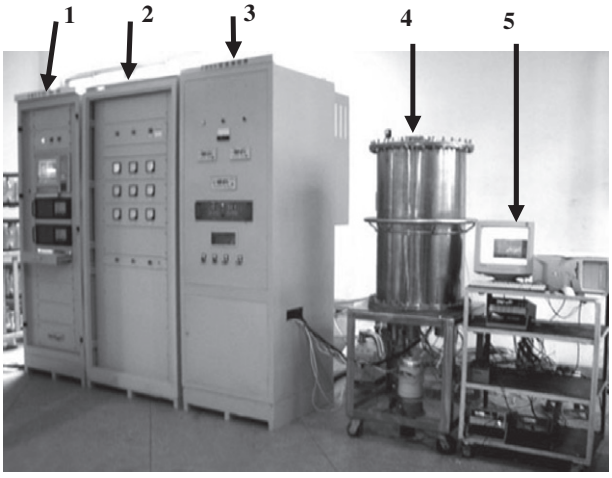

1- monitor and control system 2- power conditioning system

3- monitor of cooling system

4- superconducting magnet and cooling system

5- data acquisition system for experiment

Fig. 7. 35 kJ/7 kW laboratory SMES.

is shown by Fig. 7. The SMES consists of four parts: High Temperature Superconducting magnet (HTS magnet), cooling system, Power Conditioning System (PCS) and Monitor and Control System (MCS).

The 35 kJ/7 kW HTS SMES was connected to a physical power system in the laboratory as shown by Fig. 8, where a 15 kV generator was connected to laboratory busbar through a transformer and lumped reactors (representing transmission lines). *K*5 is the point where a circuit breaker was connected to earth to apply three-phase-to-earth fault. Excitation and energy release of the magnet are controlled by the PCS. Damping control was realized on the SMES main control board and it took the active power delivered through the transformer as the feedback signal. Only experiment of damping control through controlling active power exchange with the physical power system was conducted, because the SMES was not integrated with voltage control function. Exper-

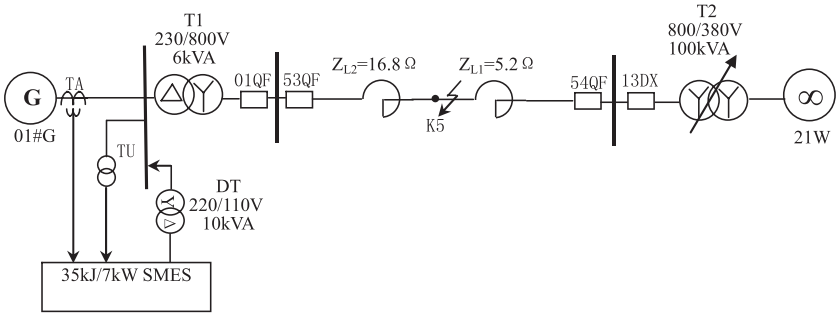

Fig. 8. Configuration of the physical power system with the SMES connected.

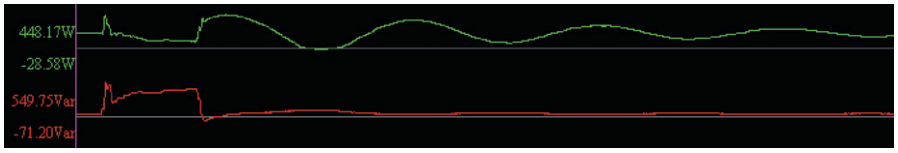

(a) Without the SMES damping control

(b) Active power output from the generator = 3000W

(c) Active power output from the generator = 4000W

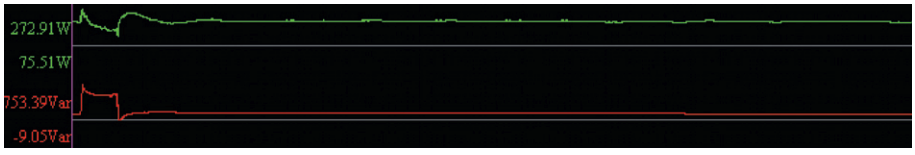

(d) Active power output from the generator = 4200W

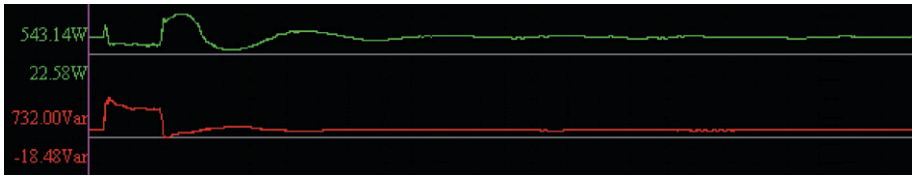

(e) Active power output from the generator = 4500W

Fig. 9. Results of laboratory experiment.

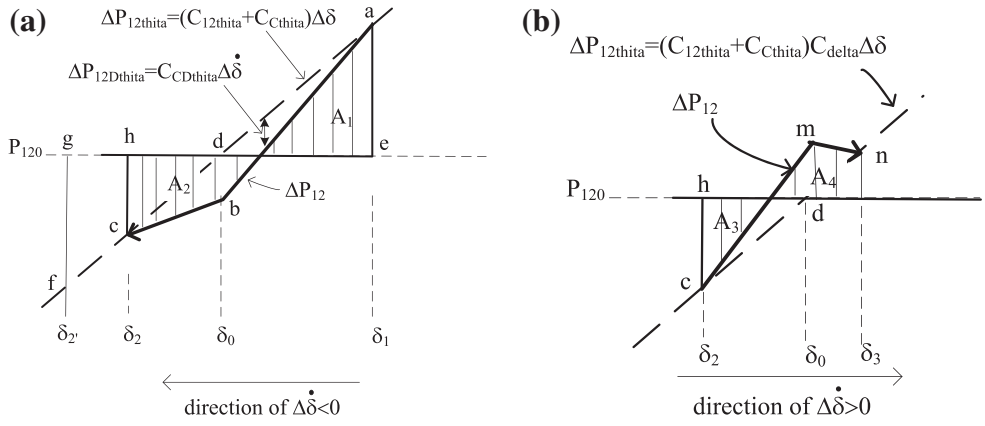

Fig. A1. Analysis of damping effect of ESS control.

imental results are given in Fig. 9, where [1]green lines are variations of active power delivered along the transmission line of the physical power system. From Fig. 9 we can see that the effectiveness of SMES damping control changed little with the variations of system load conditions. This confirmed the analytical conclusions obtained in the paper.

5. Conclusions

It has been well-known that effectiveness of conventional Power System Stabilizer (PSS) and some newly-appeared Flexible AC Transmission System (FACTS) based stabilizers, such as Static Synchronous Compensator (STATCOM) and Unified Power Flow Controller (UPFC), changes with power system operating conditions. This has brought about the long-standing and challenging problem of design of robust power system damping controllers. It has been expected that ESS damping control can be of some different special features, because ESS cannot only regulate its exchange of reactive power with power system as PSS, STATCOM and UPFC does, but also control its exchange of active power. The original contribution of this paper is the revelation of one special property of ESS damping control through theoretical analysis, confirmed by simulation study and laboratory experiment. It is concluded in the paper that ESS damping control implemented by active power regulation is robust (or at least more robust than damping control realized by regulating reactive power) to variations of power system operating conditions. Hence ESS damping control is of great potential to provide solution to the problem of robust stabilization of power system oscillations.

Work presented in the paper is based on simple case of single-machine infinite-bus power systems. It gives insight into and good understanding of the problem, which will guide further work on the case of multi-machine power systems. The proposed new analytical method is presented in the paper for a single-machine infinite-bus power system. This is the case that the proposed method is quite similar to the conventional technique of damping torque analysis. However, the proposed analytical method can be easily extended to the case of damping control by ESS to suppress power oscillation along a transmission line in a multi-machine power system [18]. This provides the possibility for the authors to investigate the robustness of ESS damping control in multi-machine power systems. The authors are well aware of the complexity of analysis when case of multi-machine power systems is looked into. They are working now on demonstration of examples of applying the proposed methods in multi-machine power systems and expect to report the results in near future. The authors also would like to point out is that work presented in this paper has not considered the limitation of ESS capacity when it is applied to suppress power system oscillations. This is also an important issue affecting the capability of ESS damping control which is under intensive investigations by the authors.

[1] Please note that Fig. 9 will appear in B/W in print and color in the web version. Based on this, please note and approve the edit in Fig. 10 caption.

Acknowledgements

The authors would like to acknowledge the support of the EPSRC UK–China joint research consortium (EP/F061242/1), the science bridge award (EP/G042594/1), UK, the Jiangsu Power Company, China, and the Fund of Best Post-Graduate Students of Southeast University, China. Prof. Haifeng Wang is a member of the international innovation team of superconducting technology for electrical engineering at the Institute of Electrical Engineering, Beijing, China, sponsored by the Chinese Academy of Sciences, China.

Appendix A

In Fig. A1a, line 'ac' is the linearization of P_{12}–δ curve for small-signal analysis that is given by Eq. (5). At the steady state, the system operates at point (δ_0, P_{120}). We assume that the small-disturbance oscillation starts from point 'a' in Fig. A1a. At point 'a', the increase of P_{12} is $\Delta P_{12thita}$ proportional to $\Delta\delta$ as shown in Eq. (4). The operating point is on the line $\Delta P_{12} = \Delta P_{12thita} = (C_{12thita} + C_{Cthita})\Delta\delta$ because at point 'a', $\Delta\dot{\delta} = 0$ and hence $\Delta P_{12Dthita} = C_{CDthita}\Delta\dot{\delta} = 0$. When the operating point moves down from 'a', because $\Delta\dot{\delta} < 0$, $\Delta P_{12Dthita} = C_{CDthita}\Delta\dot{\delta} < 0$ that will be added on $\Delta P_{12thita}$. Hence the operating point should move along the P_{12}–δ curve that is below the line $\Delta P_{12thita} = (C_{12thita} + C_{Cthita})\Delta\delta$ (assuming $C_{CDthita} > 0$). When $\Delta\dot{\delta} = 0$, the operating point stops moving and must come back to the line $\Delta P_{12thita} = (C_{12thita} + C_{Cthita})\Delta\delta$ at point 'c' where $\Delta P_{12Dthita} = C_{CDthita}\Delta\dot{\delta} = 0$. Without $\Delta P_{12Dthita} = C_{CDthita}\Delta\dot{\delta}$, area 'ade' should be equal to area 'dgf' that will lead to $|\delta_1| = |\delta_2|$. With $\Delta P_{12Dthita} = C_{CDthita}\Delta\dot{\delta}$ being added, not only area 'ade' is reduced to A_1 but also extra area is generated below the line $\Delta P_{12thita} = (C_{12thita} + C_{Cthita})\Delta\delta$ to form area A_2. Hence $A_2 = A_1$ must lead to $|\delta_2| < |\delta_1| = |\delta_2|$, which indicates that the oscillation is damped due to the existence of the term $\Delta P_{12Dthita} = C_{CDthita}\Delta\dot{\delta}$.

In Fig. 10b, at operating point 'c', the accelerating area actually formed is 'cdh' that is smaller than A_2 in Fig. 3a. Furthermore, when the operating point moves up, it moves above the line $\Delta P_{12} = \Delta P_{12thita} = (C_{12thita} + C_{Cthita})\Delta\delta$ due to the extra term $\Delta P_{12Dthita} = C_{CDthita}\Delta\dot{\delta} > 0$ because $\Delta\dot{\delta} > 0$. Hence the accelerating area is A_3 that is even smaller than area 'cdh'. A similar analysis can be carried out

for the operating point to move up along P_{12}–δ curve above the line $\Delta P_{12thita} = (C_{12thita} + C_{Cthita})\Delta\delta$, leading to $|\delta_3| < |\delta_2|$ as it is shown in Fig. 3c, indicating the oscillation is damped. In addition, from the analysis we can see that the higher the proportional coefficient $C_{CDthita}$ is, the more $|\delta_i|$ ($i = 2, 3$) decreases that means the better damping effect is achieved by ESS control.

Appendix B

From Eq. (1) we have $V_{td} + jV_{tq} = jX(I_{tsd} + jI_{tsq}) + V_d + jV_q$.

Because $V_{td} = X_q I_{tsq}, V_{tq} = E'_q - X'_d I_{tsd}$

$$I_{tsq} = \frac{V\sin\theta}{X_q + X} = \frac{bV_b\sin\delta + aV_c\sin(\delta-\gamma)}{X_{q\Sigma}},$$

$$I_{tsd} = \frac{E'_q - V\cos\theta}{X'_d + X} = \frac{E'_q - bV_b\cos\delta - aV_c\cos(\delta-\gamma)}{X'_{d\Sigma}}$$

From Fig. 1 we have $V_{td} + jV_{tq} = jX(I_{tsd} + jI_{tsq}) + V_{sd} + jV_{sq}$ and hence

$$V_{sd} = X'_{ts\Sigma} I_{tsq} = \frac{X'_{ts\Sigma}}{X'_{\Sigma}}[bV_b\sin\delta + aV_c\sin(\delta-\gamma)]$$

$$V_{sq} = V_{tq} - X_{ts}I_{tsd} = E'_q - (X'_d + X_{ts})I_{tsd} = E'_q - \frac{X'_{dts\Sigma}}{X_{d\Sigma}}(E'_q - V\cos\theta)$$

$$= \frac{X'_{d\Sigma} - X'_{dts\Sigma}}{X'_{d\Sigma}}E'_q + \frac{X'_{dts\Sigma}}{X'_{d\Sigma}}[bV_b\cos\delta + aV_c\cos(\delta-\gamma)]$$

That gives

$$\Delta V_{sd} = \frac{X_{ts\Sigma}}{X'_{d\Sigma}}[bV_{b0}\cos\delta_0 + aV_{c0}\cos(\delta_0-\gamma_0)]\Delta\delta + \frac{X_{ts\Sigma}}{X'_{d\Sigma}}aV_{c0}\sin(\delta_0 - \gamma_0)\Delta V_c - \frac{X_{ts\Sigma}}{X'_{d\Sigma}}aV_{c0}\cos(\delta_0-\gamma_0)\Delta\gamma$$

$$\Delta V_{sq} = -\frac{X'_{dts\Sigma}}{X'_{d\Sigma}}[bV_{b0}\sin\delta_0 + aV_{c0}\sin(\delta_0-\gamma_0)]\Delta\delta + \frac{X'_{dts\Sigma}}{X'_{d\Sigma}}aV_{c0}\cos(\delta_0 - \gamma_0)\Delta V_c + \frac{X'_{dts\Sigma}}{X'_{d\Sigma}}aV_{c0}\sin(\delta_0-\gamma_0)\Delta\gamma$$

So we can have

$$\Delta V_s = \frac{1}{V_{s0}}(V_{sd0}\Delta V_{sd} + V_{sq0}\Delta V_{sq}) = C_1\Delta\delta + C_2\Delta V_c + C_3\Delta\gamma \qquad (A1)$$

Appendix C

Transmission line: $X_{ts} = 0.3$ p.u., $X_{sb} = 0.3$ p.u., $X_s = 0.3$ p.u.

Generator: $X_d = 0.8$ p.u., $X_q = 0.4$ p.u., $X'_d = 0.2$ p.u., $M = 8$ s., $D = 2.35$ p.u., $T'_{d0} = 5$ s.

AVR: $T_A = 0.01$ s. $K_A = 100$ p.u.

Initial load condition: $V_{t0} = 1.0$ p.u., $V_{s0} = 1.0$ p.u., $V_{b0} = 1.0$ p.u., $P_{ts0} = 0.5$ p.u.

Dynamic model of the installed BESS in [9] is used.

References

[1] Challenges of energy storage technology. Panel report of American physical society; 2007. <http://www.aps.org/policy/reports/popa-reports/upload/Energy-2007-Report-ElectricityStorageReport.pdf>.

[2] Ribeiro PF, Johnson BK, Crow ML, Arsoy A, Liu Y. Energy storage systems for advanced power applications. IEEE Proc 2001;89(12):1744–56.

[3] Hajizadeh A, Golkar MA. Control of hybrid fuel cell/energy storage distributed generation system against voltage sag. Int J Electr Power Energy Syst 2010;32(5):488–97.

[4] Mitani Y, Tauji K, Murakami Y. Application of superconducting magnet energy storage to improve power system dynamic performance. IEEE Trans Power Syst 1988;3(4):1418–25.

[5] Hsu CS, Lee WJ. Superconducting magnetic energy storage for power system applications. IEEE Trans Ind Appl 1993;29(5):990–6.

[6] Rogers JD, Boenig HJ, Bronson JC, Colyer DB, Hassenzahl WV, Turner RD, et al. 30-MJ superconducting magnetic energy storage (SMES) unit for stabilizing an electric transmission systems. IEEE Trans Magn 1979;15(1):820–3.

[7] Rahim AHMA, Mohammad AM. Improvement of synchronous generator damping through superconducting magnetic energy storage systems. IEEE Trans Energy Convers 1994;9(4):736–42.

[8] Simo JB, Kamwa I. Exploratory assessment of the dynamic behaviour of multimachine system stabilized by a SMES unit. IEEE Trans Power Syst 1995;10(3):1566–71.

[9] Arabi S, Kundur P. Stability modelling of storage devices in FACTS applications. IEEE PES Summer Meet 2001;2:767–71.

[10] Yang Z, Shen C, Zhang L, Crow M, Atcitty S. Integration of a StatCom and a battery energy storage. IEEE Trans Power Syst 2001;16(2):254–60.

[11] Kobayashi K, Goto M, Wu K, Yokomizu Y, Matsumura T. Power system stability improvement by energy storage type STATCOM. In: 2003 IEEE power tech conference proceedings, vol. 2, Bologna; 23–26 June, 2003.

[12] Li Gang, Cheng Shijie, Wen Jinyu, Pan Yuan, Ma Jia. Power system stability enhancement by a double-fed induction machine with a flywheel energy storage system. In: 2006 IEEE proceedings of power engineering society general meeting; 18–22 June, 2006.

[13] Tsang MW, Sutanto D. ANN controlled battery energy storage system for enhancing power system stability. In: 2000 International conference on advances in power system control, operation and management, APSCOM-00, vol. 2; October–November, 2000. p. 327–31.

[14] Tsang MW, Sutanto D. Power system stabiliser using energy storage. IEEE PES Winter Meet 2000;2:1354–9.

[15] Bhargava B, Dishaw G. Application of an energy source power system stabilizer on the 10 MW battery energy storage system at Chino substation. IEEE Trans Power Syst 1998;13(1):145–51.

[16] Kuwabara T, Shibuya A, Furuta H. Design and dynamic response characteristics of 400 MW adjustable speed pumped storage unit for Ohkawachi power station. IEEE Trans Energy Convers 1996;11(2):376–84.

[17] Modeling of power electronics equipment (FACTS) in load flow and stability programs. CIGRE T F 38-01-08; 1998.

[18] Song YH, Johns AT. Flexible AC transmission systems. IEE Press; 1999.